Title
STOCHASTIC ACCELERATION BY A SINGLE WAVE IN A MAGNETIC FIELD

Authors
Smith, Gary R.
Kaufman, Allan N.

Publication Date
1975-01-16

Submitted to Physical Review Letters

LBL-3242
Preprint c.1

STOCHASTIC ACCELERATION BY A SINGLE WAVE IN A MAGNETIC FIELD

Gary R. Smith and Allan N. Kaufman

January 16, 1975

Prepared for the U. S. Atomic Energy Commission
under Contract W-7405-ENG-48

DISCLAIMER

STOCHASTIC ACCELERATION BY A SINGLE WAVE IN A MAGNETIC FIELD

Gary R. Smith and Allan N. Kaufman

Department of Physics and Lawrence Berkeley Laboratory
University of California, Berkeley, California 94720

January 16, 1975

ABSTRACT

The nature of a particle orbit in an electrostatic plasma wave is modified by a magnetostatic field, because there exists a set of resonant parallel velocities $(\omega + \ell\Omega)/k_z$. If the wave amplitude Φ_o is sufficiently large, neighboring resonant regions overlap, and the particle motion becomes stochastic; the threshold condition is $k_z^2(e/m)\,\Phi_o|J_\ell(k_\perp\rho)| \approx \Omega^2/16$. As an application, a weakly damped intermediate-frequency ion-acoustic wave may be used to heat the tail of an ion distribution.

The character of the resonant interaction of a particle with an electrostatic wave can be qualitatively different in the presence or absence of an ambient magnetostatic field. In its absence, it is well known[1] that particles whose velocity (projected along the wave vector) differs from the wave phase velocity ω/k by less than the trapping half-width $2(e\Phi_o/m)^{\frac{1}{2}}$ may be trapped into orbits oscillating about the phase velocity at a bounce frequency $k(e\Phi_o/m)^{\frac{1}{2}}$. This behavior, whose short-term consequence is Landau damping, asymptotically limits the net damping and energy (or momentum) transfer of the wave to the resonant particles.

In a magnetized plasma, an electrostatic wave propagating at an oblique angle $\theta = \tan^{-1}(k_\perp/k_z)$ to the uniform field $B_o\hat{z}$ has a set of resonant parallel velocities $\{V_\ell\}$ which satisfy

$$\omega - k_z V_\ell = -\ell\Omega , \qquad \ell = 0,\pm1,\pm2,\cdots, \tag{1}$$

where the left side is the Doppler-shifted wave frequency and the right side is an integer multiple of the gyrofrequency $\Omega = eB_o/mc$. As shown below, the trapping half-width at the ℓth resonance is

$$w_\ell \equiv 2|e\Phi_o J_\ell(k_\perp\rho)/m|^{\frac{1}{2}} , \tag{2}$$

where ρ is the gyroradius of the particle. When the wave amplitude Φ_o is so large that the trapping layers $(V_\ell \pm w_\ell)$ overlap, a particle can move from one resonance region to the next, executing a random walk in v_z-space, so to speak. As a result, the mean net momentum transfer to the particles can be appreciably larger than expression (2) would indicate. In this paper we study the transition from "adiabatic"[2] particle trajectories, when Φ_o is small, to "stochastic" trajectories, when Φ_o is large. A rough criterion for the transition is given in (17). The motion of a particle in a magnetic field and a single oblique wave has previously been treated by Fredricks.[3] Analogous studies on cyclotron heating in a mirror field[4] and on "super-adiabaticity"[5] may be mentioned.

In the wave frame, moving at $(\omega/k_z)\hat{z}$ with respect to the plasma, the particle Hamiltonian is

$$H(\vec{r},\vec{p}) = \frac{1}{2m}\left(\vec{p} - \frac{eB_o}{c}x\,\hat{y}\right)^2 + e\Phi_o\sin(k_z z + k_\perp x) . \tag{3}$$

With the canonical transformation generated by

$$S(x,y;\ P_1,P_2) = xP_1 + yP_2 - P_1P_2/m\Omega \quad , \tag{4}$$

the Hamiltonian becomes

$$H(z,p_z;\ Q_1,P_1;\ P_2) = \frac{1}{2m}\left[p_z^{\ 2} + P_1^{\ 2} + (m\Omega Q_1)^2\right]$$
$$+ e\Phi_o \sin\left[k_z z + k_\perp(Q_1 + P_2/m\Omega)\right] \quad , \tag{5}$$

where $P_1 = p_x$, $P_2 = p_y$, and $Q_1 = x - P_2/m\Omega$. Since (5) does not depend on Q_2, P_2 is a constant of the motion which we can set to zero, by choice of the origin $x = 0$. We then use another canonical transformation, generated by

$$S'(Q_1;\ \phi) = \frac{1}{2} m\Omega Q_1^{\ 2} \cot\phi \quad , \tag{6}$$

to write the Hamiltonian as

$$H(z,p_z;\ \phi,p_\phi) = p_z^{\ 2}/2m + \Omega p_\phi + e\Phi_o \sin\left[k_z z - k_\perp \rho \sin\phi\right], \tag{7}$$

where $Q_1 = -\rho\sin\phi$, and $p_\phi = \left[P_1^{\ 2} + (m\Omega Q_1)^2\right]/2m\Omega$ is the canonical angular momentum of gyration, conjugate to the gyrophase ϕ. We use the convenient abbreviation $\rho \equiv (2p_\phi/m\Omega)^{\frac{1}{2}}$, the gyroradius. This Hamiltonian system has two degrees of freedom. Since (7) is independent of time, in the wave frame the energy of the particle is conserved.

To analyze (7), it is helpful to use the Bessel function identity

$$\exp(ik_\perp \rho \sin\phi) = \sum_{\ell=-\infty}^{\infty} J_\ell(k_\perp \rho)\exp(i\ell\phi) \tag{8}$$

to write (7) as

$$H = p_z^{\ 2}/2m + \Omega p_\phi + e\Phi_o \sum_\ell J_\ell(k_\perp \rho)\sin(k_z z - \ell\phi) \quad . \tag{9}$$

If the wave amplitude is small enough we can treat the last term in (9) as a small perturbation of the unperturbed Hamiltonian

$$H_o(p_z,p_\phi) = p_z^{\ 2}/2m + \Omega p_\phi \ . \tag{10}$$

The zeroth-order equations of motion derived from (10) yield

$$v_z \equiv \dot{z} = p_z/m \ , \quad \dot{\phi} = \Omega \ , \quad p_z = \text{const} \ , \quad p_\phi = \text{const}. \tag{11}$$

Substituting

$$z = v_z t + z_o \ , \quad \phi = \Omega t \tag{12}$$

into the last term of (9) yields

$$H \approx H_o(p_z,p_\phi) + e\Phi_o \sum_{\ell=-\infty}^{\infty} J_\ell(k_\perp \rho)\sin\left[(k_z v_z - \ell\Omega)t + k_z z_o\right] \ . \tag{13}$$

When one of the resonance conditions[6]

$$k_z v_z - \ell\Omega \approx 0 \tag{14}$$

is satisfied, the motion is dominated by a <u>single</u> term of the sum over ℓ for times much longer than Ω^{-1}. The exact Hamiltonian (9) can then be approximated by

$$H_\ell \equiv H_o(p_z,p_\phi) + e\Phi_o J_\ell(k_\perp \rho)\sin(k_z z - \ell\phi) \quad , \tag{15}$$

for which a constant of the motion (in addition to the energy) exists:

$$I_\ell \equiv p_\phi + \ell p_z/k_z \ . \tag{16}$$

When the wave amplitude is not small, the above analysis breaks down, and we might expect no additional constant of the motion to exist. By using the exact Hamiltonian (7) we have found that the constant of the motion does indeed disappear fairly abruptly as the wave amplitude increases.

To visualize the disappearance of the constant of the motion we use the "surface of section" method. (This method has been used to analyze several other nonlinear oscillator systems.[7] For present purposes, we view it as a technique for representing the four-dimensional phase-space trajectory in two dimensions, so we can draw it on paper.) To construct the surface of section plots, the trajectory is calculated numerically using the Hamiltonian equations. We look at a cross section ($\phi = \pi$) of phase space, and see the trajectory represented by dots in a three-dimensional space. We then project the dots onto a two-dimensional surface to obtain a surface of section plot. If the dots lie on a curve, an additional constant of the motion exists. If the dots fill an area, the energy is the only constant of the motion. The sample plot in Fig. 1 was generated using Hamiltonian (7). In this case the dots, which represent the coordinates of the particle at intervals of the gyroperiod, are projected onto the zp_z-plane. In some regions of the plane, which we call "adiabatic," initial conditions lead to dots lying on a curve. In the other regions of the plane, which we call "stochastic," initial conditions lead to dots filling an area. Figure 1 illustrates the power of this method for exhibiting the extent of adiabatic and stochastic regions, and also for revealing other types of complexity in the particle motion. We do not yet completely understand all the features appearing in Fig. 1.

The condition for the onset of stochastic particle motion can be derived using the method of Walker and Ford.[8] We refer to the plot shown in Fig. 2, for which the wave amplitude is smaller than for Fig. 1, and all initial conditions lead to adiabatic particle motion. Notice the similarity in appearance of each of the three curves to the phase space orbit of a trapped particle in an unmagnetized plasma.[1] In the magnetized case, the curves shown in Fig. 2 are near the separatrices which surround the resonance conditions (14) for $\ell = 0, \pm 1$. From (15), we see that the trapping half-widths are given by (2). As the wave amplitude increases, these widths increase. The additional constant of the motion will cease to exist, and particle motion will change from adiabatic to stochastic, when two separatrices touch. We may then expect the particle to be able to move from the vicinity of one resonance to the vicinity of another. This occurs when $(w_{\ell+1} + w_\ell)$, the sum of neighboring half-widths, equals the resonance separation $|V_{\ell+1} - V_\ell| = \Omega/k_z$; i.e., roughly when

$$\omega_\ell/\Omega \approx \frac{1}{4} , \tag{17}$$

where $\omega_\ell \equiv k_z w_\ell/2$ is the bounce frequency at the ℓth resonance. This crude estimate is in good agreement with our numerical results, which show a transition from adiabatic to stochastic particle motion when the wave amplitude Φ_o is increased through the value given by (17).

When the wave amplitude is large enough that particle motion is stochastic, the particle distribution may be significantly heated by the interactions with the wave. The evolution of the distribution resembles a diffusion process in velocity space. These results are illustrated in Fig. 3, which shows a sequence of three surface of section plots of increasing wave amplitude. In these plots the trajectory dots have been projected onto the $v_\perp v_z$-plane instead of the zp_z-plane. Eight initial conditions were used to generate each of the plots: the initial conditions all have the same values of the velocity $(k_z v_{\perp o}/\Omega = k_\perp \rho_o = 2.24,\ k_z v_{zo}/\Omega = -3.6)$ and gyrophase $(\phi_o = \pi)$, but different values of z_o. This set of initial conditions corresponds to a ring distribution (in the plasma frame)

$$f(v_z, v_\perp) = \frac{1}{2\pi\, v_{\perp o}}\, \delta(v_z)\, \delta(v_\perp - v_{\perp o}) \tag{18}$$

when $\omega = 3.6\ \Omega$. In the case of small wave amplitude $\left[(\tilde{\omega}/\Omega)^2 \equiv k_z^2 |e\Phi_o|/m\Omega^2 = 0.25\right]$, all initial conditions led to adiabatic motion; the velocity of a particle changed little from its initial value. In the case of large wave amplitude $\left[(\tilde{\omega}/\Omega)^2 = 0.75\right]$, all initial conditions led to stochastic particle motion, and the time-averaged values of both perpendicular and parallel velocities (in the plasma frame) increased significantly. The transition from adiabatic to stochastic motion corresponds to an increase of wave amplitude by a factor of three. The results shown in Fig. 3 indicate the transition at about $(\tilde{\omega}/\Omega)^2 = 0.50$. In order to compare this result to (17) we use $\ell = -3$ because $k_z v_{zo}/\Omega = -3.6$ is between the resonances $\ell = -3$ and -4, and for the parameters of Fig. 3 the half-width w_{-3} is several times w_{-4}. The numerically observed threshold condition is thus

$$(\tilde{\omega}/\Omega)^2 |J_\ell(k_\perp \rho)| = (0.50)|J_{-3}(2.24)| \approx \frac{1}{12}, \tag{19}$$

which is remarkably close to (17), considering the crude theory used.

To illustrate the application of these concepts, we choose a particular wave, the "intermediate-frequency acoustic"[9] wave, propagating with angle $\theta = 45^\circ$ between the wave vector and magnetic field.

This longitudinal wave has the dispersion relation $\omega \approx kc_s$, very similar to an ion-acoustic wave in an unmagnetized plasma. To be specific (and consistent with Fig. 3) we choose $\omega = 3.6\ \Omega$ and $T_e/T_i = 16$. Then $\omega/k_z = 6.2\ v_i$, where v_i is the ion thermal speed, so there is negligible ion Landau damping. Further, there is negligible linear ion-cyclotron-harmonic damping: the thermal ions (shown by cross-hatching in Fig. 3) can have $\ell = -3$ and $\ell = -4$ resonances, but the damping is proportional to $\Lambda_\ell(\beta) \equiv I_\ell(\beta)\exp(-\beta)$, and with $k_\perp v_i/\Omega \equiv \beta^{\frac{1}{2}} \approx 0.58$, we see that $\Lambda_3(0.34) \approx 5\times 10^{-4}$ and $\Lambda_4(0.34) \approx 3\times 10^{-5}$ are quite small. We now examine ions in the Maxwell tail, specifically, at $v_z = 0$ (in the plasma frame) and $k_\perp \rho = 2.24$ $(v_\perp \approx 3.8\ v_i)$, which are just the initial conditions used in Fig. 3. These ions will be accelerated by the wave when $(\tilde{\omega}/\Omega)^2 \geq 0.50$, that is, when $e\Phi_o \geq \frac{3}{2} T_i$. An acoustic wave with $e\Phi_o = \frac{3}{2} T_i = \frac{1}{11} T_e$ has a density amplitude $\delta n/n \approx \frac{1}{13}$ and a wave energy density $\omega\, \partial\varepsilon/\partial\omega \langle E^2\rangle/8\pi \approx nT_i/15$, and is thus in the linear regime. We have shown the possiblity of heating the tail of the ion distribution, by an intermediate-frequency acoustic wave of frequency ω a few times the gyrofrequency Ω, propagating at an oblique angle, and of a certain minimum amplitude given by (17).

We acknowledge useful discussions with S. Johnston, D. Nicholson, B. Cohen, M. Mostrom, C. Birdsall, J. Harte, W. Nevins, A. Lichtenberg, and G. Johnston. This work was supported in part by the U.S. Atomic Energy Commission and by an NSF Graduate Fellowship held by one of the authors (GRS).

FOOTNOTES AND REFERENCES

1. T. M. O'Neil, Phys. Fluids 8, 2255 (1965).
2. The terms "adiabatic" and "stochastic" have come into use to characterize phase-space orbits that are respectively stable or unstable with respect to an infinitesimal variation of initial conditions. We avoid the term "ergodic" for an unstable orbit, as the orbit does not fill the whole energy hypersurface, but only a part of it.
3. R. W. Fredricks, J. Plasma Phys. 1, 241 (1967). That paper used different methods and obtained different results.
4. F. Jaeger, A. J. Lichtenberg and M. A. Lieberman, Plasma Phys. 14, 317 (1972).
5. R. E. Aamodt, Phys. Rev. Lett. 27, 135 (1971); M. N. Rosenbluth, Phys. Rev. Lett. 29, 408 (1972); A. V. Timofeev, Nucl. Fusion 14, 165 (1974).
6. Note that $\omega = 0$ in the wave frame, so that (14) is the same condition as (1).
7. See references in G. M. Zaslavskii and B. V. Chirikov, Usp. Fiz. Nauk 105, 3 (1971) (Sov. Phys.-Uspekhi 14, 549 (1972)); and J. Ford, Adv. Chem. Phys. 24, 155 (1973).
8. G. H. Walker and J. Ford, Phys. Rev. 188, 416 (1969).
9. T. E. Stringer, Plasma Phys. 5, 89 (1963), has used this terminology to distinguish the present wave from acoustic waves with frequencies either less than the ion gyrofrequency or greater than the electron gyrofrequency. Also see A. B. Mikhailovskii, Theory of Plasma Instabilities (Consultants Bureau, N.Y., 1974), Vol. I, Chap. 8, p. 148.

FIGURE CAPTIONS

Fig. 1. Sample surface of section plot. The symbol A indicates one of the adiabatic regions, S one of the stochastic regions. Curves have been drawn to connect the dots lying in adiabatic regions. The dashed lines represent the limitations on the particle motion due to conservation of energy. The parameters have the fixed values $k_\perp \rho_E \equiv k_\perp (2E/m)^{\frac{1}{2}}/\Omega = 1.48$, $(\tilde{\omega}/\Omega)^2 \equiv k_z^{\,2}|e\Phi_o|/m\Omega^2 = 0.1$, $\theta = 45^\circ$. The 15 initial conditions used to generate the dots are shown by X's. A chain of five islands is indicated by the numbers 1,2,3,4,5.

Fig. 2. Surface of section plot showing trajectory dots resulting from initial conditions near the three accessible resonances, $\ell = 0, \pm 1$. The parameters have the same values as in Fig. 1 except $(\tilde{\omega}/\Omega)^2 = 0.025$.

Fig. 3. Three surface of section plots illustrating the transition from adiabatic to stochastic particle motion and the onset of heating as the wave amplitude is increased. The values of $(\tilde{\omega}/\Omega)^2$ are shown; the energy parameter has the value $k_\perp \rho_E = 4.24$ and $\theta = 45^\circ$. The initial conditions correspond to the ring distribution (18). The dashed lines represent the limitations on the particle motion due to conservation of energy in the wave frame. The axis showing v_z in the plasma frame is based on $\omega = 3.6\ \Omega$. The numbers 0,1,2,5,6,7 on the last plot show the coordinates of the particle initially and at the ends of the corresponding gyroperiods. On the first plot cross-hatching shows the extent of the thermal ions considered in the wave-heating example.

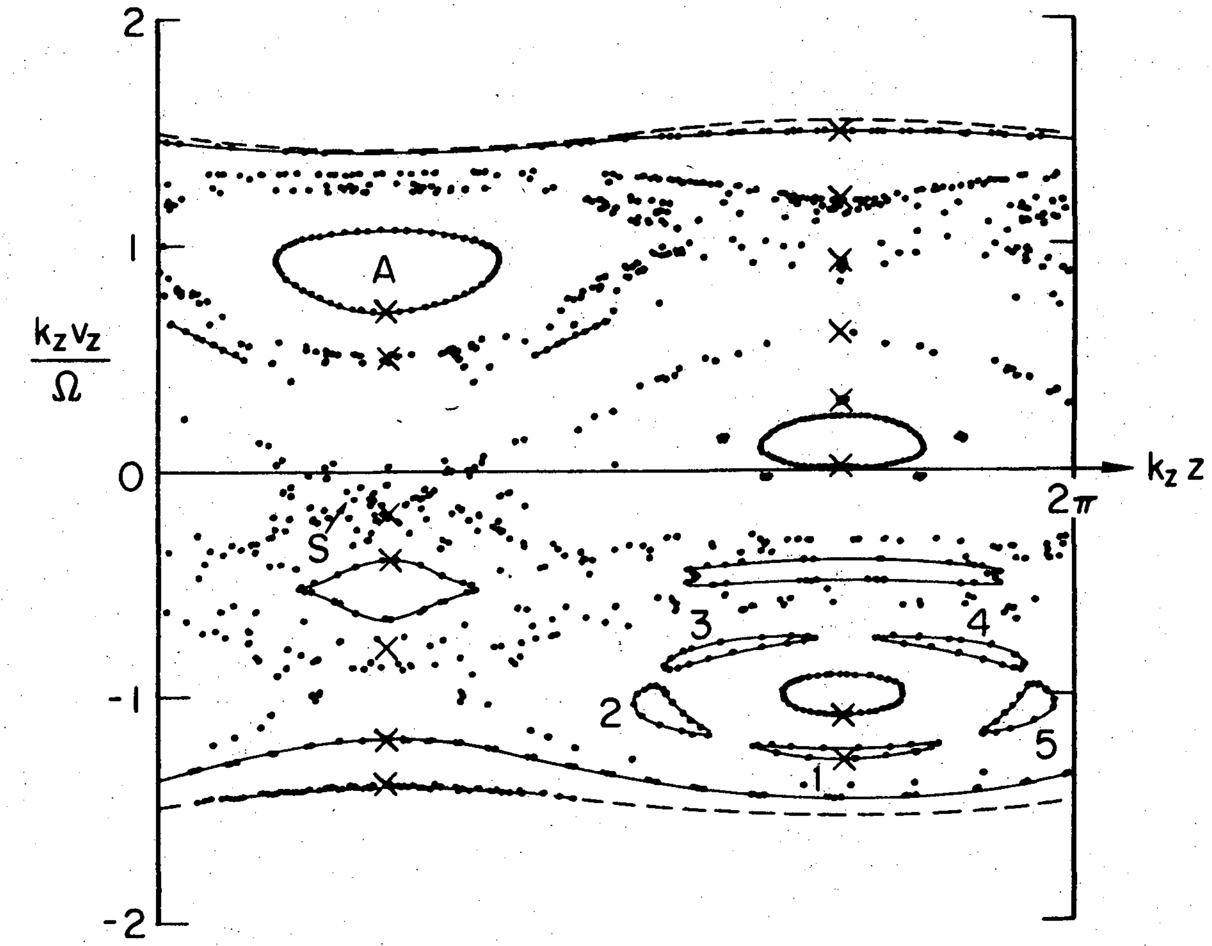

XBL751-2046

Fig. 1.

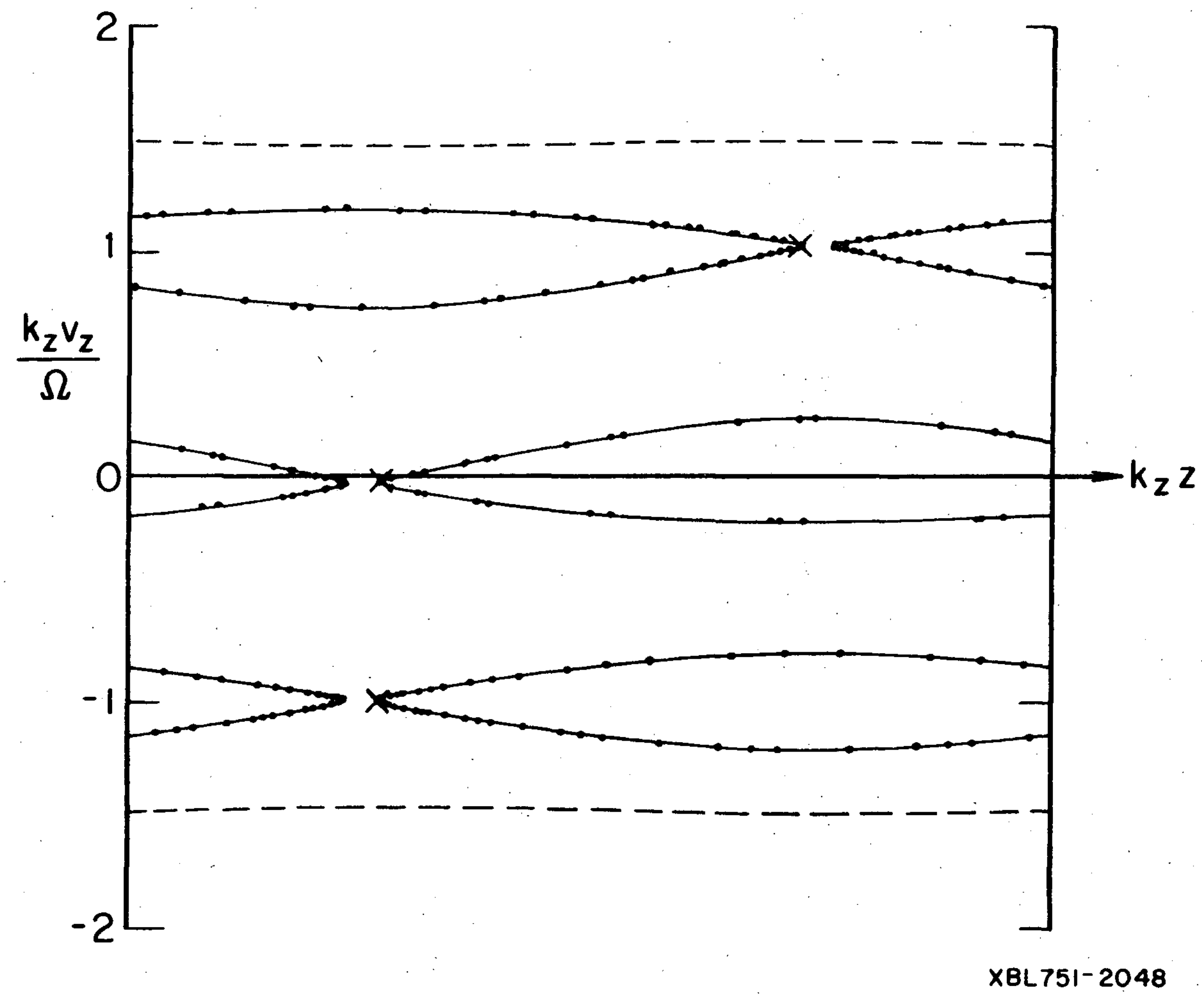

Fig. 2.

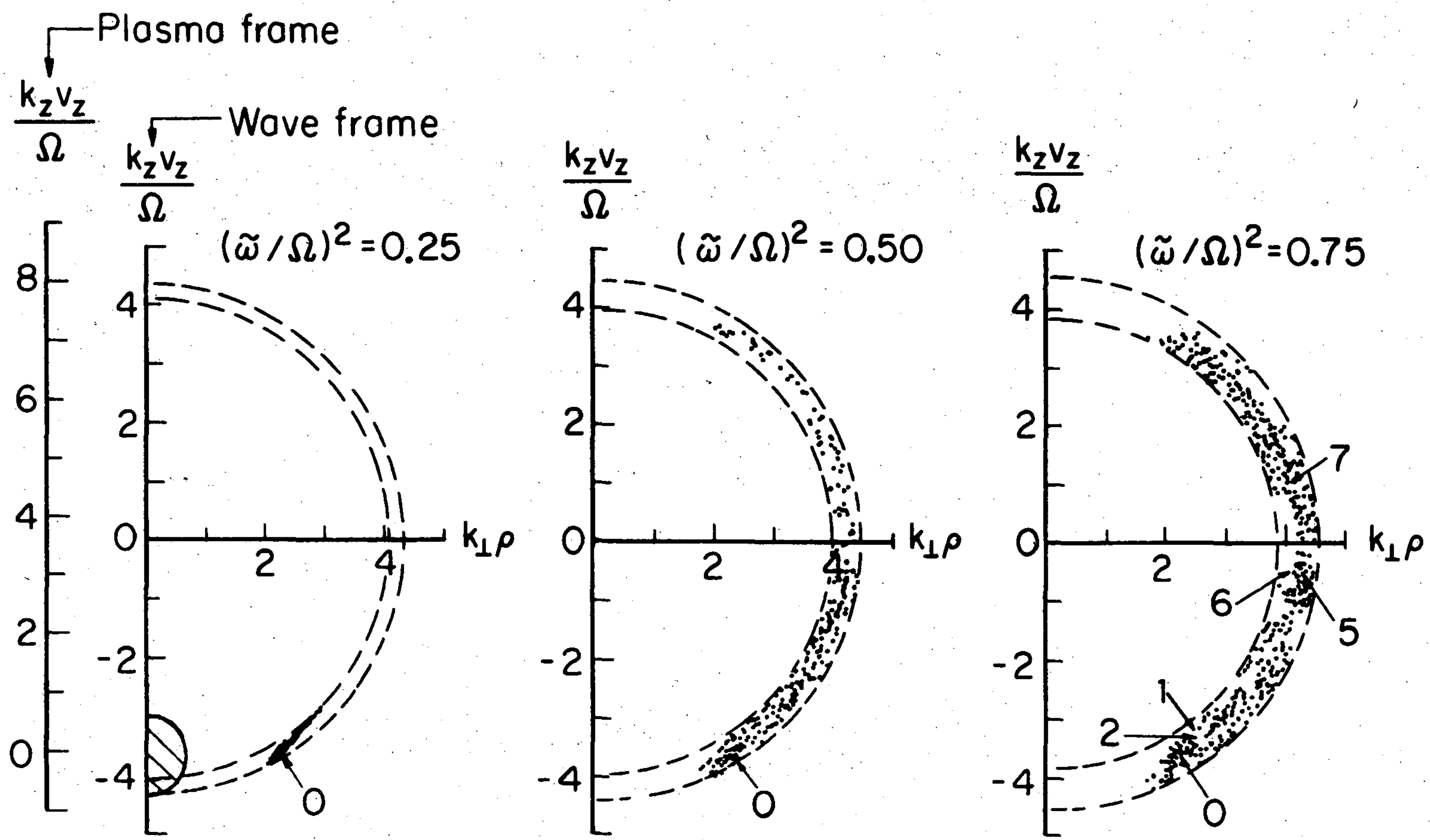
Plasma frame
Wave frame
$\frac{k_z v_z}{\Omega}$
$(\tilde{\omega}/\Omega)^2=0.25$
$(\tilde{\omega}/\Omega)^2=0.50$
$(\tilde{\omega}/\Omega)^2=0.75$
$k_\perp \rho$
XBL751-2047

Fig. 3.

TECHNICAL INFORMATION DIVISION
LAWRENCE BERKELEY LABORATORY
UNIVERSITY OF CALIFORNIA
BERKELEY, CALIFORNIA 94720